Investigation of Single Photon Emission Computed Tomography Acquired on Helical Trajectories

Maximilian P. Oppelt, James C. Sanders, Andreas Maier

Pattern Recognition Lab, FAU Erlangen-Nuremberg
maximilian.oppelt@fau.de

Abstract. This study compares the quality of single photon emission computed tomography images obtained using step-and-shoot and helical trajectories. Monte Carlo simulations of an extended phantom on both trajectories were performed using a parallel hole collimator. Standard filtered-backprojection was used for reconstruction. Both trajectories collected data for the same amount of time. Corresponding to equivalent useful acquisition times, the background signal-to-noise ratios and sphere to background contrasts were roughly equivalent in both reconstructions. However, the helical trajectory requires 20% less true acquisition time due to the elimination of delay due to detector repositioning. Helical trajectories in SPECT can thus reduce overall acquisition time while having negligible effects on image quality.

1 Introduction

Single photon emission computed tomography (SPECT) is a nuclear imaging modality that provides three-dimensional functional information of different tissues. It utilizes distribution properties of radioactive tracers injected into the human body to image processes such as blood perfusion and metabolism and aid in the detection of tumors or other pathologies. During a tomographic scan, the detector is rotated about the patient in discrete steps, with time loss between projections during which no data are acquired. Additionally, a translation of the bed between circular rotations is required if the anatomical region of interest exceeds the detector's axial field of view.

This procedure, referred to as step-and-shoot here, is standard in clinical applications and has several limitations. The most obvious of these is the time loss between projections, which may approach three seconds in a commercial system. Another drawback is the overlap required by adjacent bed positions to limit artifacts that may occur during the connection, or *zipping*, of neighboring reconstructions. This overlap requires extra rotations, and, together with the time loss between projections, requires the patient to endure a longer time within in the imaging device.

In 1993, Weng et al. originally introduced an approach for reconstructing helical cone-beam SPECT images [1], the primary motivation for which was

H. Handels et al. (Hrsg.), *Bildverarbeitung für die Medizin 2015,* Informatik aktuell,
DOI 10.1007/978-3-662-46224-9_86,

the fulfillment of data sufficiency conditions. Despite the utility of cone-beam SPECT, most of the clinical imaging systems use parallel projection geometry and thus circumvent the data sufficiency issues associated with cone-beam collimation. Subsequent work focused on the sister modality of Positron Emission Tomography (PET), where groups such as Townsend et al. in [2] and Braun et al. in [3] proposed whole body spiral PET with continuous bed motion and extension to PET/MR, respectively. Both authors showed equivalent to slightly better statistical properties due to improved axial uniformity, and indicated that time savings were possible due to elimination of discrete bed translations. Braun et al. also concluded that continuous bed motion brings a higher flexibility in simultaneous PET and MR whole-body data acquisition. In SPECT imaging, a variant of continuous detector rotation was proposed by Cao et al. in [4], where a rough equivalence between it and standard step-and-shoot was shown.

The goal of this work is to investigate the feasibility of using continuous detector and bed motion in SPECT imaging to provide equivalent image quality in less total acquisition time. To accomplish this, we employ a novel helical acquisition trajectory and compare it to step-and-shoot using Monte Carlo simulations. The results of these simulations, as well as a discussion and outlook, are presented below.

2 Materials and methods

2.1 Experimental data and simulation

A voxelized cylinder phantom with radius 22 pixels and axial length 192 pixels was created, and two sets of six spheres with diameters of 6.5, 5.2, 4.1, 3.2, 2.6, 2.1 pixels in a hexagonal formation were centered in axial planes 96 and 160 (Fig. 1). The spheres were given a contrast of 5:1 relative to the rest of the cylinder to emulate hot objects in a warm background. With a virtual pixel size of 4.8 mm, they represent respective volumes of 16, 8, 4, 2, 1 and 0.5 ml found in the commonly used Jaszczak phantom.

We used the SIMIND Monte Carlo simulation program to generate SPECT projection data [5], where the detector was rotated, and the phantom shifted

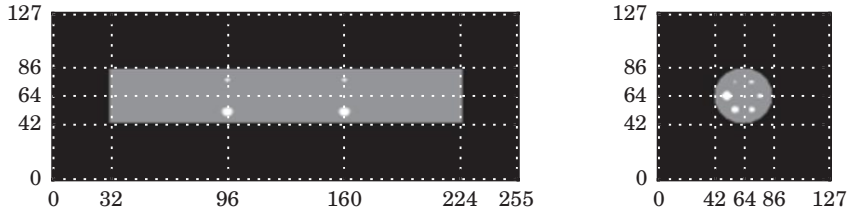

(a) Axial view (b) Transversal view

Fig. 1. Transversal and axial view of the phantom source density map.

between projections to emulate various acquisition trajectory parameters. The detector had axial and transverse dimensions of 64 and 128 pixels, respectively, and the pixel size was matched to the phantom's at 4.8 mm. A single detector head outfitted with a low energy high resolution, parallel hole collimator was simulated, and all orbits were circular with a radius of 25 cm. Projections were scaled and Poisson noise incorporated to achieve realistic noise levels that would be obtained if the phantom were loaded with 700 MBq of ^{99m}Tc and acquired for dwell times discussed below. The effects of scatter and attenuation were neglected in this preliminary investigation

2.2 Acquisition trajectories

Our proposed acquisition trajectory in Fig. 2(a) consists of one circular continuous rotation with no bed movement followed by a pair of continuous helix rotations with a constant forward bed speed. This is then followed by a second circular rotation at the opposite end of the phantom and concludes with two continuous helix rotations with a constant reverse bed speed. The rotation speed is constant, and each complete orbit lasts 900 seconds, throughout which data are acquired, thus yielding a total useful acquisition time of 90 minutes. Our

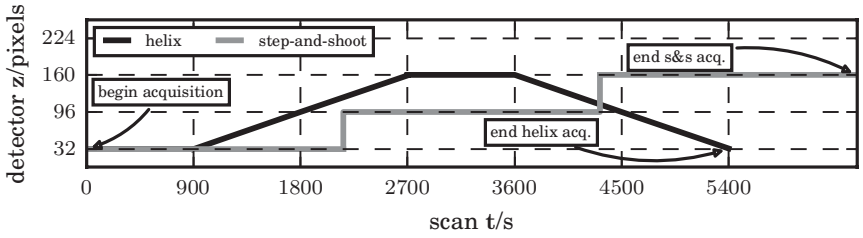

(a) Detector position versus true acquisition time

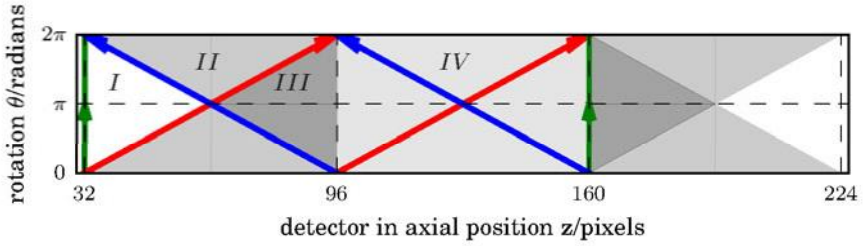

(b) Angular sampling for continuous camera motion

Fig. 2. Acquisition details for step-and-shoot (a) and continuous camera motion (b), where the bold lines indicate the axial position of the first row of the detector (green: circle, red: forward helix, blue: reverse helix). Shading indicates the degree of coverage for each position in sinogram space. (I): circular rotation, (II): circular and either forward or reverse helical, (III) circular, forward and reverse helical, (IV) forward and reverse helix.

simulated projection duration was 2.5 seconds, which provided 360 projections for each rotation.

Fig. 2(b) shows the resulting coverage in sinogram space. The white areas *I)* are only scanned once with a circular trajectory, lightly shaded areas (*II* and *IV*) are scanned twice with either a combination of circular and helical or two helical rotations, respectively. Darkly shaded regions (*III*) are scanned three times, with a circular and both forward and reverse helical orbits.

In order to compare the results of our helical scan to the standard step and shoot case, we performed a second simulation incorporating orbits of 120 projections over a 360 degree arc at three axial positions. The projection time was set to the 15 seconds often used in clinical situations, yielding a total useful acquisition time equivalent to the helix case. In practice, roughly three seconds is spent rotating the camera between projections, leading to the longer total acquisition time reflected by the light gray curve in Fig. 2(a). The overlap between axial positions used in clinical situations was neglected.

2.3 Reconstruction and evaluation

To reconstruct our helical trajectory, we rebinned the acquired data into a pseudo-step and shoot sinogram. Our sinogram is binned in 360 steps for a full rotation, and for each angle in the sinogram the columns of the detector are interpolated to a 128x64 pixel gird. If one pixel is measured multiple times, the average is computed. Reconstruction of the sinograms was carried out using the standard filtered-backprojection method with a ramp filter [6].

For evaluation, we computed the contrast in the spheres relative to a region in the center of the phantom. We also computed the signal to noise ratio (SNR) in each homogeneous phantom slice. This was defined as follows: $SNR = \frac{\mu_{sig}}{\sigma_{bg}}$.

3 Results

The reconstructed results are shown in Fig. 3. Visual inspection indicates the image quality within the phantom to be roughly equivalent, although streaking artifacts outside the cylinder are more apparent in the step-and-shoot case.

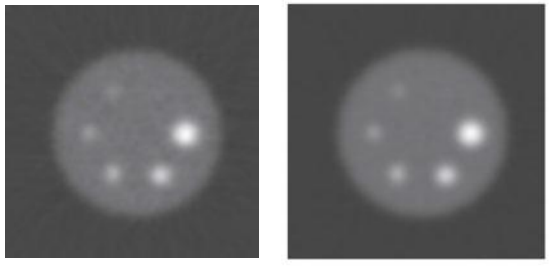

(a) Step and Shoot (b) Helical

Fig. 3. Filtered backprojection of slices with spheres within volume.

Table 1. Sphere to background contrasts for source map (C_{src}), helix (C_{helix}) and step-and-shoot ($C_{\mathrm{S\&S}}$) acquisition trajectories. The average value for a given sphere size over the two sets is reported.

D(pixels)	C_{src}	C_{helix}	$C_{\mathrm{S\&S}}$
6.5	5.0	4.36	4.21
5.2	5.0	3.64	3.56
4.1	5.0	2.91	2.91
3.2	5.0	2.25	2.26
2.6	5.0	1.77	1.75
2.1	5.0	1.19	1.27

Sphere contrast appears equal, and the smaller spheres suffer from partial volume effects caused by the collimator's point spread function. Visual impressions in the spheres are confirmed by the contrasts reported in Tab. 1, which show no significant difference between the two methods.

The SNR is shown for each axial position in Fig. 4, where the helix acquisition yields slightly better noise characteristics, potentially corresponding to a reduction in streaking artifacts within the phantom. Nevertheless, this difference is very small and subjectively difficult to discern in the images. A slight dip in helix acquisition's SNR is visible at both ends of the phantom corresponding to the areas of single coverage indicated in Fig. 2(b).

4 Discussion

We have shown that for an acquisition on helical trajectories with both continuous bed and detector motion, the image quality is approximately equivalent to the case of an analogous step-and-shoot trajectory. Both acquisitions yield the same *useful* acquisition time for acquiring data, but the step-and-shoot case requires approximately 20% more *true* acquisition time for detector repositioning. In practice, axial overlap is required by step-and-shoot methods to prevent reconstruction artifacts, leading to even more time losses relative to our proposed helix acquisition.

This time saving could be further increased by using statistical iterative reconstruction methods like Maximum Likelihood Expectation Maximization,

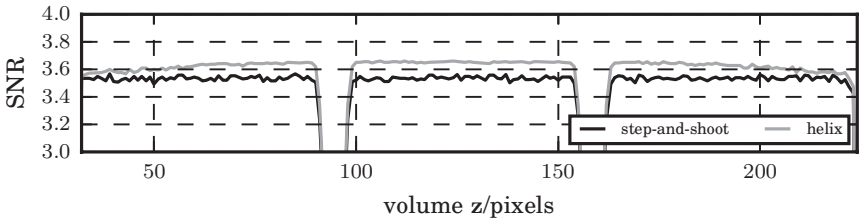

Fig. 4. SNR at each axial position in the phantom. The metric was not computed in slices containing spheres, hence the pair of dips in the curves.

which circumvent the angular sampling requirement of filtered backprojection and would allow one to shorten the circular rotations at the ends of the phantom. We can also think of varying the speed of axial and rotational motion during the acquisition to have more control over the temporal resolution and statistical properties of the acquisition.

However, the study is not without limitations. Specifically, our simulation method assumed a stationary volume during each 2.5 second projection. However, for a true acquisition with continuous bed and detector motion, the volume would be translated by 0.85 mm, and rotated by one degree during this time, leading to a finite amount of blurring. In SPECT imaging, resolution loss due to relatively large detector pixel sizes and wide point spread functions (both on the order of several millimeters) may dominate this blurring, but its characterization would become important for higher-resolution systems or faster acquisition trajectories. Additionally, we did not consider the physical effects of scatter and attenuation, which are a further image quality impediment in SPECT imaging.

4.1 Conclusion

Using helical trajectories in SPECT saves *true* acquisition time, while maintaining the image quality of traditional step-and-shoot protocols. In this experiment, we observed no adverse effects of a helical trajectory, but this conclusion must be qualified by our exclusion of physical factors such as detector movement during the projection, attenuation, and scatter. Nevertheless, our results motivate further investigation of SPECT acquisition on helical trajectories and a more thorough characterization of the aforementioned effects excluded here.

References

1. Weng Y, Zeng G, Gullberg G. A reconstruction algorithm for helical cone-beam SPECT. IEEE Nucl Sci Symp Conf Rec. 1993;40(4):1092–101.
2. Townsend DW, Reed J, Newport DF, et al.; IEEE. Continuous bed motion acquisition for an LSO PET/CT scanner. IEEE Nucl Sci Symp Conf Rec. 2004;4:2383–7.
3. Braun H, Ziegler S, Lentschig MG, et al. Implementation and performance evaluation of simultaneous PET/MR whole-body imaging with continuous table motion. J Nucl Med. 2014;55(1):161–8.
4. Cao Z, Maunoury C, Chen CC, et al. Comparison of continuous step-and-shoot versus step-and-shoot acquisition SPECT. J Nucl Med. 1996;37(12):2037–40.
5. Ljungberg M, Strand SE. A Monte Carlo program for the simulation of scintillation camera characteristics. Comput Methods Programs Biomed. 1989;29(4):257–72.
6. Bracewell RH, Riddle AC. Inversion of fan beam scans in radio astronomy. Astrophys J. 1967;150:427–34.